Rana A. K. Al-Refaia,[1] Zainab Shakir Abdullah Al-Ali,[2]* Eman Alrikabi,[1]
Ahmed Ali Alkarimi,[1] and Fatmah M. Alkhatib[3]

[1]Department of Chemistry, College of Sciences, University of Babylon. Babylon, Iraq. sci.rana.abdul@uobabylon.edu.iq, alrikabieman@gmail.com, sci.ahmed.ali@uobabylon.edu.iq.
[2]Department of Chemistry, College of Sciences, University of Basrah. Basrah, Iraq. zainab.abdulah@uobasrah.edu.iq.
[3]Department of Chemistry, Faculty of Science, Umm Al-Qura University. Makkah, Saudi Arabia. fmkhatib@uqu.edu.sa.

*Corresponding author: zainab.abdulah@uobasrah.edu.iq.

Received: 21/07/2025. **Last review:** 08/09/2025. **Accepted:** 26/11/2025.

Organic and Biochemistry

Biogenic Synthesis of Multifunctional Zinc Oxide Nanoparticles Using *Rosmarinus officinalis* L. Extract: Comprehensive Evaluation of Antibacterial, Antioxidant, and Antimalarial Potential

Abstract

This study reports an eco-friendly synthesis of zinc oxide nanoparticles (ZnO-NPs) using *Rosmarinus officinalis* L. leaf extract as a reducing and stabilizing agent. The extract was characterized by Fourier Transform Infrared (FT-IR) and Gas Chromatography-Mass Spectrometry (GC-MS). The biosynthesized ZnO-NPs were thoroughly characterized through UV-Vis spectroscopy showing a distinctive absorption peak at 372 nm, FT-IR confirms phytochemical capping, XRD reveals hexagonal wurtzite structure with crystallite size of 42.47 ± 1.20 nm, and SEM/EDX exhibits spherical morphology with high purity. The ZnO-NPs exhibited dose-dependent antibacterial activity against *Staphylococcus aureus* (24.0 ± 0.5 mm at 100 µg/mL) and *Escherichia coli* (18.0 ± 0.3 mm), outperforming the crude extract. Antioxidant assays, with ascorbic acid (vitamin C) as a positive control, demonstrated 89.2 ± 2.1% DPPH inhibition (IC_{50} = 28.4 µg/mL), comparable to ascorbic acid. Notably, ZnO-NPs showed 82.3 ± 3.2% β-haematin inhibition (50 µM), surpassing chloroquine (68.1 ± 2.8%), suggesting antimalarial potential. These findings highlight their potential as multifunctional therapeutic agents with a novel and promising antimalarial application.

Keywords: Ecological synthesis; Antibacterial activity; Therapeutic nanoparticles.

Síntesis biogénica de nanopartículas multifuncionales de óxido de zinc a partir de extracto de *Rosmarinus officinalis* L.: evaluación integral del potencial antibacteriano, antioxidante y antipalúdico

Resumen

Este estudio presenta una síntesis ecológica de nanopartículas de óxido de zinc (ZnO-NPs) utilizando extracto de hojas de *Rosmarinus officinalis* L. como agente reductor y estabilizante. El extracto se caracterizó mediante FTIR y GC-MS. Las ZnO-NPs biosintetizadas se caracterizaron exhaustivamente mediante espectroscopia UV-Vis, que mostró un pico de absorción característico a 372 nm; FT-IR, que confirmó el recubrimiento fitoquímico; XRD, que reveló una estructura hexagonal de wurtzita con un tamaño de cristalito de 42,47 ± 1,20 nm; y SEM/EDX, que mostró una morfología esférica con alta pureza. Las nanopartículas exhibieron actividad antibacteriana dosis-dependiente contra *Staphylococcus aureus* (24,0 ± 0,5 mm a 100 µg/mL) y *Escherichia coli* (18,0 ± 0,3 mm), superando al extracto crudo. Los ensayos antioxidantes, con ácido ascórbico (vitamina C) como control positivo, demostraron una inhibición del DPPH del 89,2 ± 2,1% (IC_{50} = 28,4 µg/mL), comparable a la del ácido ascórbico. Cabe destacar que las nanopartículas de ZnO mostraron una inhibición de la β-hematina del 82,3 ± 3,2% (50 µM), superando a la cloroquina (68,1 ± 2,8%), lo que sugiere un potencial antipalúdico. Estos hallazgos resaltan su potencial como agentes terapéuticos multifuncionales con indicación para una aplicación antipalúdica novedosa y prometedora.

Palabras clave: síntesis ecológica; actividad antibacteriana; nanopartículas terapéuticas.

Síntese biogénica de nanopartículas multifuncionais de óxido de zinco utilizando extrato de *Rosmarinus officinalis* L.: avaliação abrangente do potencial antibacteriano, antioxidante e antimalárico

Resumo

Este estudo reporta uma síntese ecológica de nanopartículas de óxido de zinco (ZnO-NPs) utilizando extrato da folha de *Rosmarinus officinalis* L. como agente redutor e estabilizante. O extrato foi caracterizado por FTIR e GC-MS. As ZnO-NPs biossintetizadas foram completamente caracterizadas por espectroscopia UV-Vis apresentando um pico de absorção distinto a 372 nm, FT-IR confirmando o capeamento fitoquímico, XRD revelando estrutura hexagonal wurtzita com um tamanho de cristalito de 42,47 ± 1,20 nm e SEM/EDX exibindo morfologia esférica com elevada pureza. As NPs exibiram atividade antibacteriana dose-dependente contra *Staphylococcus aureus* (24,0 ± 0,5 mm a 100 µg/mL) e *Escherichia coli* (18,0 ± 0,3 mm), superando o extrato bruto. Os ensaios antioxidantes, utilizando o ácido ascórbico (vitamina C) como controlo positivo, demonstraram uma inibição de 89,2 ± 2,1% do DPPH (CI_{50} = 28,4 µg/mL), comparável ao ácido ascórbico. Notavelmente, as NPs de ZnO apresentaram uma inibição de 82,3 ± 3,2% da β-hematina (50 µM), superando a cloroquina (68,1 ± 2,8%), sugerindo potencial antimalárico. Essas descobertas destacam seu potencial como agentes terapêuticos multifuncionais com indicação para uma nova e promissora aplicação antimalárica.

Palavras-chave: síntese ecológica; atividade antibacteriana; nanopartículas terapêuticas.

Introduction

Nanotechnology has enabled the widespread use of biodegradable nanoparticles, which exhibit diverse morphologies, including spherical, rod-shaped, needle-like, and crystalline structures [1, 2]. Conventional physical and chemical synthesis methods, however, has environmental and biological risks due to their toxicity and high costs. To address these limitations, green synthesis approaches —particularly biosynthesis— have gained prominence as sustainable and efficient alternatives [3–5].

The selection of an appropriate plant source is critical, as the specific phytochemical profile directly influences the reduction, nucleation, and stabilization processes during nanoparticle formation [6]. For example, *Rosmarinus officinalis* L. (rosemary) is a medicinal plant renowned for its rich composition of bioactive compounds, including polyphenols (e.g., rosmarinic acid, caffeic acid), flavonoids, and terpenoids (e.g., 1,8-cineole, camphor, α-pinene) [7]. These phytochemicals are particularly effective in green synthesis; the polyphenols and flavonoids act as potent reducing agents for metal salt precursors, while the terpenoids and long-chain fatty acids serve as effective capping and stabilizing agents, preventing nanoparticle aggregation and controlling their final size and morphology [8].

Biosynthesized metal nanoparticles, especially those derived from plant extracts, demonstrate significant therapeutic potential against bacterial, fungal, and dermatological infections [9, 10]. Among various metal oxides, zinc oxide nanoparticles (ZnO-NPs) have attracted considerable attention due to their cost-effective production, biocompatibility, and unique physicochemical properties, including high photostability, broad-spectrum light absorption, and strong electrochemical activity [11–13]. They are effective against drug-resistant pathogens due to mechanisms such as the production of reactive oxygen species (ROS), the release of Zn^{2+} ions, and direct cellular internalization [14].

The emergence of bacteria that are resistant to multiple drugs, including methicillin-resistant *Staphylococcus aureus* and *Escherichia coli*, has intensified the search for alternative antimicrobial agents. Metal nanoparticles (MNPs), including silver, gold, copper, and ZnO-NPs, offer promising solutions by leveraging their intrinsic antibacterial properties, which reduce the likelihood of resistance development [15–17]. Additionally, phototherapeutic strategies like photothermal and photodynamic therapies, which utilize MNPs to generate heat or ROS, present non-antibiotic approaches to combat infections while minimizing resistance risks [18].

Beyond antimicrobial applications, MNPs exhibit enzyme-mimetic antioxidant properties, scavenging free radicals and mitigating oxidative stress-related diseases [9, 10]. Their efficacy depends on factors such as size, surface charge, and chemical composition [8, 19]. Certain oxide nanoparticles can neutralize reactive nitrogen and oxygen species by converting alkyl peroxyl radicals into stable hydroperoxides, further highlighting their therapeutic potential [20].

MNPs also show promise in combating malaria, targeting both the Plasmodium parasite and its mosquito vector. Studies emphasize the role of silver, gold, and palladium nanoparticles in early-stage infection control [21, 22], while copper nanoparticles have also demonstrated antimalarial activity [23]. This study aims to develop a green synthesis method for ZnO-NPs using *Rosmarinus officinalis* L. extract. For this purpose, the physicochemical properties of the nanoparticles were characterized and their antibacterial activity against multidrug-resistant bacteria (MDR) strains were evaluated, recognizing their antioxidant potential through free radical scavenging assays, and, for the first time, identifying their antimalarial efficacy via inhibition of beta-haematin formation.

Materials and Methods

All chemicals and reagents were purchased from Sigma-Aldrich, while *Rosmarinus officinalis* L. leaf was purchased from a local Iraqi market.

Preparation of Rosmarinus officinalis L. *Leaf Extract*

Fresh leaves of *Rosmarinus officinalis* L. were purchased from a Babylonian local market; 10 g of leaves were successively washed three times with distilled water and once with a 75:25 *v*/*v* ethanol-water solution to decontaminate their surfaces. After being cleaned, the leaves were oven-dried for 24 h at 70 °C. Using a mortar and pestle, the dried material was ground into a fine powder. 8 g of the powdered leaves were refluxed in 100 mL of distilled water at 80 °C for 60 min while being continuously stirred by a magnetic stirrer set at 600 rpm to prepare the extract. Whatman No. 1 filter paper was used to filter the resultant mixture, and the filtrate was kept at 4 °C until it was needed again.

Biosynthesis of Zinc Oxide Nanoparticles (ZnO-NPs)

ZnO-NPs were synthesized through a modified green synthesis approach. In a typical procedure, 100 mL of the prepared leaf extract was combined with 100 mL of 0.5 M zinc acetate dihydrate solution under constant stirring. Subsequently, 80 mL of 0.5 M NaOH solution was added dropwise to the mixture. The reaction was maintained at room temperature with continuous stirring (600 rpm) for 3 h, during which a yellowish precipitate formed. The obtained precipitate was collected by vacuum filtration and subjected to multiple washing cycles with both distilled water and ethanol to remove residual impurities. The purified product was then calcined at 400 °C for 60 min, yielding a light-yellow powder. The final product was ground to uniform consistency and stored in airtight containers for subsequent characterization and applications [24].

Antimicrobial Susceptibility Testing

The antibacterial efficacy of the biosynthesized ZnO-NPs was evaluated against representative Gram-positive (*Staphylococcus aureus*) and Gram-negative (*Escherichia coli*) bacterial strains using the agar well diffusion method. Bacterial suspensions were standardized to 0.5 McFarland turbidity and uniformly swabbed onto Mueller-Hinton agar plates. Wells (6 mm diameter) were aseptically punched into the agar, into which 100 µL of test solutions (10 µg/mL concentration of either ZnO nanoparticles or plant extract) were dispensed. Following 24 h incubation at 37 °C, the zones of inhibition were measured using calibrated calipers. All experiments were performed in triplicate under sterile conditions.

Antioxidant Activity Evaluation

DPPH Radical Scavenging Assay

The free radical scavenging capacity was determined using the 2,2-diphenyl-1-picrylhydrazyl (DPPH) method with modifications [25, 26]. Test samples (ZnO-NPs and ascorbic acid standard) at concentrations ranging from 10-100 µg/mL were mixed with 1 mL of methanolic DPPH solution (1 mM). After vortexing, the reaction mixtures were incubated in the dark at room temperature for 30 min. Absorbance measurements were recorded at 517 nm using a spectrophotometer. The radical scavenging activity was calculated as:

$$\%\ \text{of DPPH Scavenged} = \frac{\text{Ab of control} - \text{Ab of test}}{\text{Ab of control}} \times 100 \qquad (1)$$

Where Ab of control represents the absorbance of DPPH solution without test and Ab of test denotes the absorbance of the test solution.

Hydrogen Peroxide H_2O_2 Scavenging Assay

The ability to neutralize hydrogen peroxide (H_2O_2) was evaluated by mixing 0.1 mL of ZnO-NPs solution (25 – 250 µg/mL in 50 mM phosphate buffer, pH 7.4) with 0.6 mL of 2 mM H_2O_2 solution and 0.3 mL of phosphate buffer. Following 10 min of incubation, absorbance was measured at 230 nm. Ascorbic acid served as the positive control [27]. The scavenging activity was determined as:

$$\% \text{ Hydrogen peroxide scavenging activity} = \frac{Ac - As}{Ac} \times 100 \quad (2)$$

Where Ac is the control's absorbance and As is the absorbance of ZnO-NPs or vitamin C.

Hydroxyl Radical (OH•) Scavenging Assay

The hydroxyl radical (OH•) scavenging activity was evaluated by Keshari *et al.* [27]. A mixture of 0.075 mL of ZnO-NPs (25–250 µg/mL in methanol), 0.45 mL of sodium phosphate buffer (200 mM, pH = 7.0), 0.15 mL of deoxyribose (10 mM), 0.150 mL of FeSO4-EDTA (10 mM), 0.15 mL of H_2O_2 (10 mM), and 0.525 mL of distilled water was prepared. The solution was then incubated for four hours. The reaction was stopped when 0.75 mL of two different concentrations of thiobarbituric acid (TBA) (2.8 and 1%) in 50 mM NaOH were added. The mixture was then heated in a boiling water bath for 10 min before cooling with tap water. Ultimately, methanol was employed as a blank, and vitamin C was used as a standard when the absorbance was measured at 520 nm. Eq. (3) was used to estimate the percentage.

$$\% \text{ Hydroxyl radical scavenging activity} = \frac{Ac - As}{Ac} \times 100 \quad (3)$$

Whereas Ac is the absorbance of the control (all the reagents except the test sample) and As is the absorbance of ZnO-NPs or vitamin C.

Superoxide Radical ($O_2^{\bullet -}$) Scavenging Assay

The superoxide radical ($O_2^{\bullet -}$) scavenging activity of ZnO-NPs was evaluated using a nicotinamide adenine dinucleotide-phenazine methosulfate-nitro blue tetrazolium (NADH-PMS-NBT) coupled reaction system [28]. In this assay, superoxide radicals were generated through the oxidation of nicotinamide adenine dinucleotide (NADH) in the presence of phenazine methosulfate (PMS), followed by their detection via nitro blue tetrazolium (NBT) reduction. The reaction mixture contained 0.2 mL of ZnO-NPs (100 – 550 µg/mL in methanol), 1 mL of Tris-HCl buffer (16 mM, pH 8.0), 1 mL of NBT (50 µM), 1 mL of NADH (78 µM), and 1 mL of PMS (10 µM). After thorough mixing, the solution was incubated for 5 min at 25 °C, and the absorbance was measured at 560 nm using a UV-Vis spectrophotometer. Ascorbic acid (vitamin C) was used as a positive control under identical conditions. The percentage inhibition of superoxide radical generation was determined using the following equation:

$$\% O_2^{\bullet -} \text{ scavenging activity} = \frac{Abc - Abs}{Abc} \times 100 \quad (4)$$

Whereas Abc is the absorbance of control and Abs is the absorption of ZnO-NPs or vitamin C.

β-haematin Inhibition Assay

A 58.4 mM haematin chloride stock solution was prepared by dissolving 16.3 mg in 0.2 M of NaOH. The solution was centrifuged at 7 × g for 15 min to remove undissolved particles, and the concentration was verified spectrophotometrically at 385 nm ($\varepsilon = 58{,}400\ M^{-1}\ cm^{-1}$ in 0.1 M NaOH) [28]. The inhibition of β-haematin formation was evaluated using a modified acetate-mediated crystallization method. Reaction mixtures contained 10 mL of haematin chloride solution and 0.56 M sodium acetate buffer (pH 5.0). The mixtures were incubated at 80 °C in a water bath with periodic sampling. At designated time points, 1 mL aliquots were removed and centrifuged (7 × g, 5 min) to pellet the formed β-haematin crystals. The extent of β-haematin formation was determined by measuring absorbance at two wavelengths: 400 nm (haematin-specific absorbance) and 700 nm (background scattering correction). The fraction of inhibited β-haematin formation was calculated as follows [29, 30]:

$$\text{Fractions} = (\text{A at 400 nm} - \text{A at 700 nm})\ \textit{control} - (\text{A at 400 nm} - \text{A at 700 nm})\ \textit{sample} \,/\, (\text{A at 400 nm} - \text{A at 700 nm})\ \textit{control} \quad (5)$$

Where A means absorbance and *control* and *sample* each have two absorbance readings: at 400 nm (haemin-specific absorbance) and at 700 nm (background scattering correction). The term (A at 400 nm – A at 700 nm) represents baseline-corrected haematin-specific absorbance.

Results and Discussions

UV-Visible Analysis

The synthesis of ZnO-NPs was initially detected by a change in the reaction mixture color. The UV spectrum displayed a slightly broad peak observed at 350 – 380 nm (**Figure 1**).

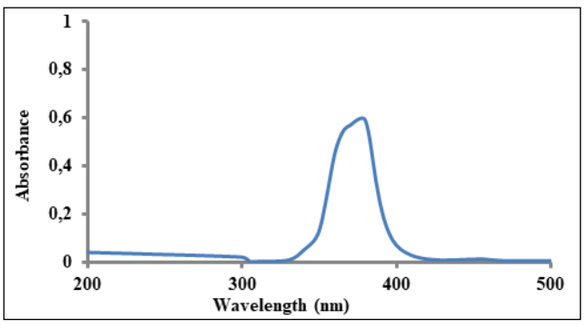

Figure 1. UV-Vis spectra of synthesized ZnO-NPs.

For ZnO-NPs, the UV-Vis spectroscopy range usually ranges from 200 to 800 nm. Because of the band gap excitation of ZnO-NPs, a distinctive absorption peak is seen within this range, typically at 350 – 375 nm. The size and synthesis technique of the nanoparticles can cause a slight shift in this peak position [31].

Fourier Transform Infrared (FT-IR) Analysis

The functional groups involved in the biosynthesis and stabilization of ZnO-NPs were characterized using fourier transform infrared (FT-IR) spectroscopy. Comparative analysis of the spectra from *Rosmarinus officinalis* L. leaf extract (**Figure 2A**) and biosynthesized ZnO-NPs (**Figure 2B**) revealed distinct vibrational patterns corresponding to various bioactive compounds. The plant extract spectrum exhibited characteristic absorption bands indicative of multiple functional groups: A broad absorption band centered at 3412.19 cm^{-1} and with a sharper peak at 3549.14 cm^{-1} were attributed to O–H stretching vibrations from phenolic compounds and carboxylic acids, along with potential N–H stretching of amine groups. Aliphatic C–H stretching vibrations appeared as a prominent band at 2931.90 cm^{-1}. The spectral region between 1587.47 and 1608.69 cm^{-1} showed strong absorption corresponding to N–H bending vibrations in primary amines. A distinct peak at 1512.24 cm^{-1} suggested the presence of amino groups (NH_2 deformation). The absorption at 1423.51 cm^{-1} was assigned to methylene group ($–CH_2–$) vibrations. Two well-defined peaks at 1257.63 and 1072.46 cm^{-1} indicated C–N stretching vibrations. The fingerprint region (600 – 650 cm^{-1}) displayed bending vibrations characteristic of C–N–C, N–C=O, and O–C=O functional groups.

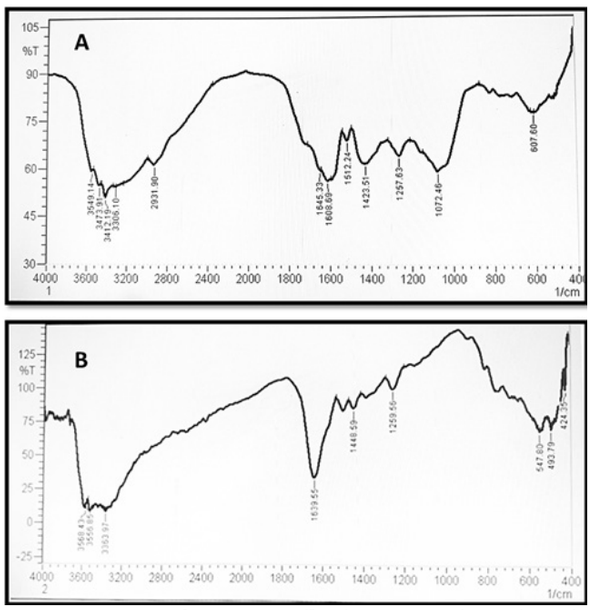

Figure 2. FT-IR spectrum of A: *Rosmarinus officinalis* L. extract and B: synthesized ZnO-NPs.

The FT-IR spectrum of the synthesized ZnO-NPs (**Figure 2B**) revealed several characteristic absorption bands. Hydroxyl and amide groups: medium-intensity peaks at 3556.85 and 3568.43 cm^{-1} correspond to O–H stretching vibrations from surface-adsorbed phenolic/alcoholic compounds and to N–H stretching of amide functional groups. Amide vibrations: a prominent absorption band at 1639.55 cm^{-1} represents the amide band I (C=O stretching). The peak at 1512.24 cm^{-1} indicates N–H bending vibrations (amide band II). Aliphatic moiety: the absorption at 1448.59 cm^{-1} is characteristic of C–H bending vibrations in methylene groups ($–CH_2–$). Carbon-nitrogen bonds: a distinct peak at 1259.56 cm^{-1} confirms the presence of C–N stretching vibrations. Zinc oxide fingerprint region: two significant peaks at 547.50 and 493.79 cm^{-1} represent the characteristic ZnO stretching vibrations, confirming successful nanoparticle formation [32].

Gas Chromatography–Mass Spectrometry (GC-MS) Analysis of Aqueous Extract of Rosmarinus officinalis L.

The resulting extract was subjected to gas chromatography–mass spectrometry (GC-MS) analysis using an Agilent Technologies 7890A instrument (USA). The GC-MS analysis revealed a phytochemical profile comprising 24 compounds related to the constitution of the rosemary aqueous extract (**Figure 3**). Using a library of common chemicals, retention duration, and mass spectra, the presence of phytochemical substances was verified.

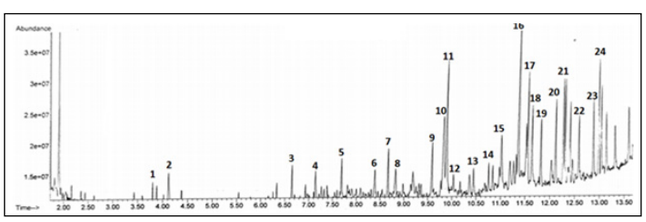

Figure 3. GC-MS chromatogram of aqueous extract of *Rosmarinus officinalis* L.

Table 1 lists the discovered chemicals along with their structures. Most are fatty acids, like cis-vaccenic acid (compound 3) and *trans*-13-octadecenoic acid (compound 20), terpenes, as α-pinene (compound 4), and phenolic derivatives like 2-methoxy-4-vinylphenol (compound 8). Notably absent were rosemary antioxidants, such as carnosic acid and rosmarinic acid, which typically require specialized detection methods such as liquid chromatography-mass spectrometry (LC–MS) analysis. The most abundant compounds were long-chain alkanes and fatty acid derivatives, with α-pinene (0.05% abundance) being the only major terpene detected. This study detected higher proportions of fatty acids (28-34 carbon chains) compared to typical rosemary profiles in consulted bibliography, suggesting extraction selectivity. The phenolic 2-methoxy-4-vinylphenol (compound 8) (0.4% here) aligns with reports of its presence in rosemary. Detected ω-7 and ω-9 fatty acids match the reports on rosemary's anti-inflammatory effects [7].

The GC-MS study spectrum elucidates the key molecules implicated in the proposed synthesis mechanism, along with interference from other substances. Numerous initiatives are underway to comprehend the mechanisms of ZnO-NPs production. Nevertheless, most studies concentrate on bioreduction through bacteria, fungi, and, particularly, plants. The GC-MS analysis identifies the key compounds and their potential roles in ZnO-NPs synthesis, particularly as reducing agents, stabilizers, and capping agents. Octadecanal (compound 2), bicyclo[3.1.1]heptane-3-one (compound 5), and benzeneethanol (compound 12) likely act as reducing agents due to their aldehyde, ketone, and alcohol functionalities, respectively.

Fatty acids (*cis*-vaccenic acid and trans-13-octadecenoic acid) and alkenes (1-heptadecene and 1-nonadecene), stabilize nanoparticles by forming protective layers. Long-chain alkanes (octadecane, 4-methyldocosane) and terpenes (α-pinene) prevent aggregation via hydrophobic interactions (capping agents). On the other hand, the phenolic compounds, 2-methoxy-4-vinylphenol (compound 8) and 1, 4-benzenediol derivative (compound 24), act as antioxidants, enhancing ZnO-NPs stability. The green synthesis of ZnO-NPs using rosemary aqueous extract can be explained through the following three-step mechanism involving reduction, nucleation, and stabilization (**Figure 4**):

1. The polar functional groups (–CHO, >C=O, –OH) which present as reducing agents in rosemary extract donate electrons to Zn^{2+} ions, reducing them to zerovalent zinc (Zn^0).

2. Zn^0 reacts with dissolved oxygen or hydroxyl ions in the solution to form ZnO nuclei. Compounds like 2-methoxy-4-vinylphenol and α-pinene modulate nucleation by controlling the release of Zn^0, preventing rapid aggregation.

3. The hydrophobic tails of fatty acids/alanes surround ZnO-NPs, while polar groups (–COOH, –OH) face outward, creating a steric barrier to produce stabilization and capping ZnO-NPs.

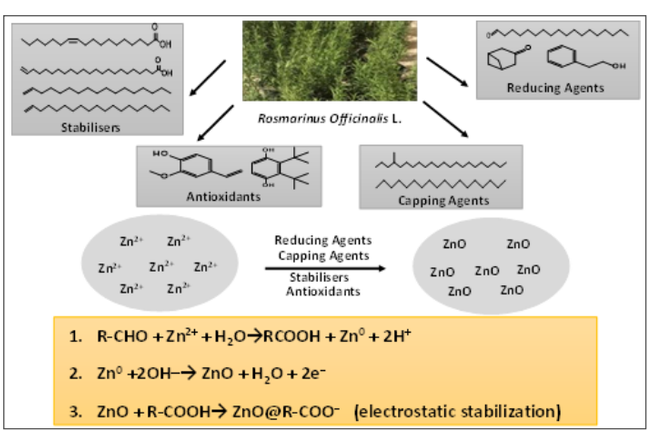

Figure 4. The suggested mechanism for the green synthesis of ZnO-NPs using aqueous extract of *Rosmarinus officinalis* L.

EDX and Scanning Electron Microscope (SEM) Analysis

Scanning Electron Microscope (SEM), Energy Dispersive X-ray Spectroscopy (EDX) and energy dispersive X-ray analysis were utilized to identify the surface morphology, size, and shape of ZnO-NPs, as shown in **Figure 5**.

Table 1. GC/MS analysis of aqueous extract of *Rosmarinus officinalis* L.

Peak	Retention time (min)	Area of peak (%)	Compound identified	Molecular formula	Molecular weight (g/mol)	Structure
1	3.80	0.04	2-Eicosanol	$C_{20}H_{42}O$	298.56	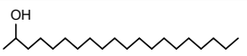
2	4.38	0.06	Octadecanal	$C_{18}H_{36}O_2$	268.49	
3	6.58	0.10	*Cis*-vaccenic acid	$C_{18}H_{34}O_2$	282.26	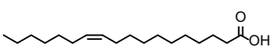
4	7.19	0.05	Bicyclo[3.1. 1]hept-2-ene(α-pinene)	C_7H_{10}	94.16	
5	7.90	0.33	Bicyclo[3.1.1]heptane-3-one	$C_7H_{10}O$	110.16	
6	8.39	0.34	4-Methyldocosane	$C_{23}H_{48}$	324.46	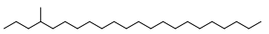
7	8.60	0.17	Cyclopropaneundecanal	$C_{14}H_{26}O$	210.36	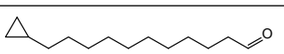
8	8.82	0.40	2-Methoxy-4-vinylphenol	$C_9H_{10}O_2$	150.18	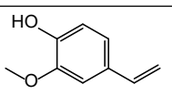
9	9.66	0.21	1-Heptadecene	$C_{17}H_{34}$	238.46	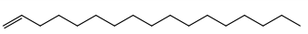
10	9.81	0.52	Oxalic acid, dodecyl isobutyl ester	$C_{18}H_{34}O_4$	314.47	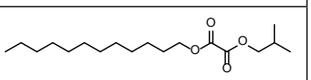
11	9.87	0.78	2, 1, 3-Benzthiadiazole	$C_6H_4N_2S$	136.17	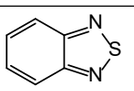
12	10.03	0.41	Benzeneethanol	$C_8H_{10}O$	122.17	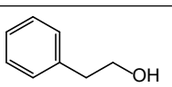
13	10.44	0.38	Octadecosane	$C_{28}H_{58}$	394.77	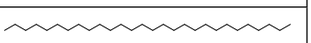
14	10.91	0.26	1- Heneicosanol	$C_{21}H_{44}O$	318.58	
15	11.19	0.53	Diethyl phthalate	$C_{12}H_{14}O_4$	222.24	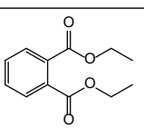
16	11.34	0.47	11,13-Dimethyl-12-tetradecen-1-ol acetate	$C_{18}H_{34}O_2$	282.47	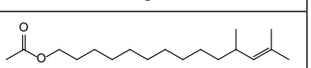
17	11.53	0.31	1-Nonadecene	$C_{19}H_{38}$	266.51	
18	11.62	0.51	1-Formyl-2,2-dimethyl-3-trane-(3-methyl-but-2-enyl)-6-methylidene-cyclohexane	$C_{15}H_{24}O$	220.36	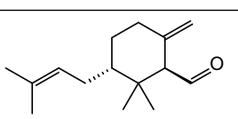
19	11.82	0.58	22-Tricosenoic acid	$C_{23}H_{44}O_2$	352.60	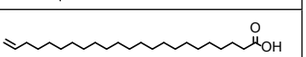
20	12.37	0.37	Trans-13-octadeceenoic acid	$C_{18}H_{34}O_2$	282.47	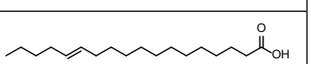
21	12.47	0.60	Octadecane	$C_{18}H_{38}$	254.50	
22	12.63	0.42	5-Methyl-z-5-docosene	$C_{23}H_{46}$	322.62	
23	12.89	0.47	1-Nonadecene	$C_{19}H_{38}$	266.51	
24	13.23	0.38	1,4-Benzenediol, bis(1,1-dimethy-lethyl)-	$C_{25}H_{45}F_5O_2$	472.63	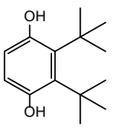

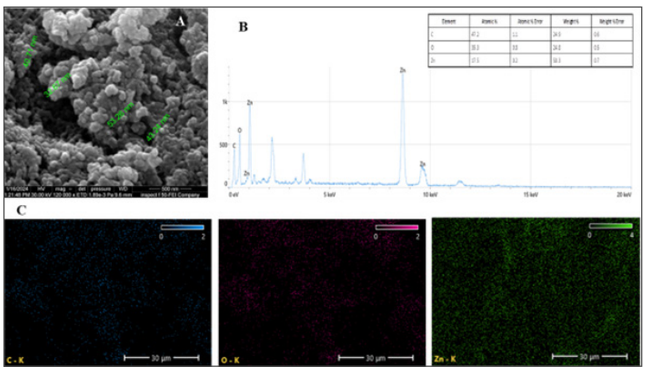

Figure 5. A: SEM imaging analysis of ZnO-NPs, B: EDX spectrum analysis of ZnO-NPs, and C: map contents.

X-ray Diffraction (XRD) Analysis

The structure has been identified as a crystallographic content notation of ($Zn_{2.00}$ $O_{2.00}$) according to Kihara and Donnay [33]. Patterns have been listed in **Table 2**.

Table 2. X-ray diffraction (XRD) pattern list.

Reference code	Score	Compound name	Displacement (°2θ)	Scale factor	Crystallographic content notation
96-900-4182	64	Zincite	0.000	0.767	$Zn_{2.00}$ $O_{2.00}$

X-ray diffraction (XRD) techniques were used to ascertain the ZnO-NPs' crystal structure and phase composition (**Figure 6**). The hexagonal structure of ZnO-NPs (JCPDS: 03-065-3411) [34] corresponds to plans 100, 002, 101, 102, 110, 103, and 112, which are the theta positions measured at 31.79, 34.28, 36.24, 47.71, 56.61, 62.71, and 68.18, according to the XRD study.

There was also background noise, which additional bioactive compounds in *Rosmarinus officinalis* L. aqueous extract may have caused. Consequently, the ZnO-NPs' crystalline nature is shown by the XRD pattern. Using Scherrer's formula, the diameter of the crystallites was calculated using the median size of 7.3 nm obtained from the X'Pert HighScore program.

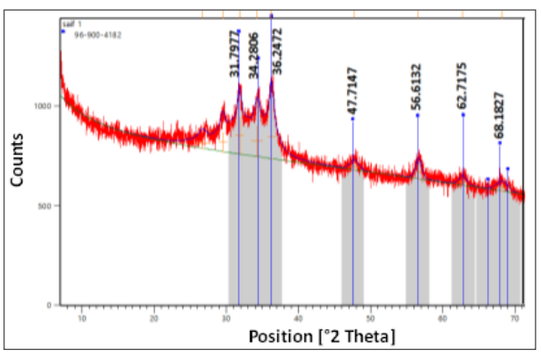

Figure 6. XRD diffraction analysis of ZnO-NPs where the peaks pointed out at 2θ values.

Antibacterial Activity

The bacteria's thick cell walls can be penetrated by ZnO-NPs, which can then disrupt their vital molecular pathways. As the bacterium cells grow larger, ZnO-NPs become more efficient in destroying them than antibiotics, to which bacteria become resistant. Osmosis penetrates the bacterial cell's interior and damages DNA, helix stability, and ribosome function, all of which eventually cause the bacterium to die [35]. On one hand, ZnO-NPs have significant antibacterial potential. Bacterial death occurs as a result of ZnO-NPs adhering to the bacterial cell wall and building up in the cytoplasm, respectively, disrupting the cell membranes. ZnO-NPs, on the other hand, function by binding to and interacting with the cell membrane in addition to building up in the lipid layer. This prevents the synthesis of enzymes, DNA, and ATP and encourages cell lysis. Furthermore, Soltanian *et al.* [36] and Sirelkhatim *et al.* [37] found that ZnO-NPs cause excessive reactive oxygen species creation and cell wall degradation.

ZnO-NPs showed good antibacterial activity against Gram-positive *S. aureus* and Gram-negative *E. coli* compared to the *Rosmarinus officinalis* L. extract at different concentrations. The inhibition zone diameters were determined against Gram-positive *S. aureus* at 7.2, 18, and 24 mm for 10, 50, and 100 µg/mL, respectively. In addition, the findings showed the inhibition zone diameters were determined against Gram-negative *E. coli* at 5, 10, and 18 mm for 10, 50, and 100 µg/mL, respectively. As shown in **Figure 7** and **Table 3**. Thus, at different concentrations of 10, 50, and 100 µg/mL, the ZnO-NPs are more effective against *S. aureus* and *E. coli* compared with *Rosmarinus officinalis* L. extract. Various processes have been proposed in some research, including direct contact between ZnO-NPs and cell walls, destruction of bacterial cell integrity, and release of antimicrobial ions, primarily Zn^{2+} ions, and generation of ROS. But aside from the physicochemical characteristics of ZnO-NPs, the toxicity mechanism changes in different media because the species of dissolved zinc (Zn) might vary depending on the components of the medium [37, 38].

Table 3. ZnO-NPs and *Rosmarinus officinalis* L. extract's inhibition zone diameter against *S. aureus* and *E. coli* at varying concentrations.

Bacteria strains	Concentration (µg/mL)	ZnO-NPs inhibition zone (mm)	*Rosmarinus officinalis* L. extract inhibition zone (mm)
S. aureus	10	7.2	0
S. aureus	50	18	0
S. aureus	100	24	7
E. coli	10	5	0
E. coli	50	10	0
E. coli	100	18	0

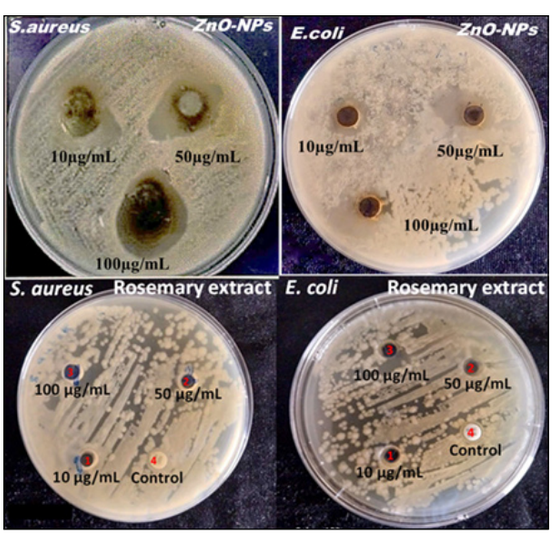

Figure 7. Antibacterial activity of ZnO-NPs and *Rosmarinus officinalis* L. extract at concentrations 10, 50, and 100 µg/mL against *S. aureus* and *E. coli*.

Antioxidant Activity

Many oxide nanoparticles can be used to treat a range of diseases linked to oxidative stress because of their physicochemical characteristics, which allow them to both exhibit antioxidant properties

and efficiently scavenge reactive nitrogen and oxygen species [39]. Chemical composition, nature, stability, surface-to-volume ratio, size, surface coating, and surface charge all influence antioxidant's characteristics. The results of this study showed that ZnO-NPs are efficient antioxidants and demonstrated strong scavenging potential against reactive oxygen species (**Figure 8**). Therefore, their capacity to transition between various oxidation states may be the cause [19].

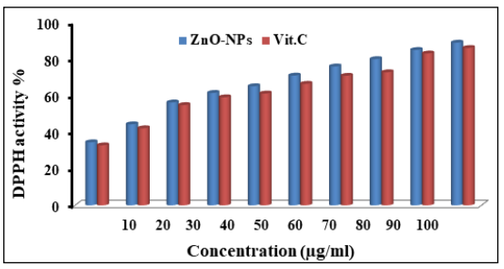

Figure 8. Activity of ZnO-NPs in 3-(3, 5-di-tert-butyl-4-hydroxyphenyl) propionic acid (DPPH) at varying concentrations compared to vitamin C.

When the DPPH assay was used, the results showed that ZnO-NPs had greater antioxidant activity than vitamin C. This observation could be explained by ZnO-NPs' surface modification of DPPH, which makes it capable of efficiently scavenging radicals. It has previously been established that DPPH and ZnO-NPs conjugate [40]. Additionally, the DPPH ZnO-NPs might make DPPH more effective at scavenging radicals that are created during the oxidation process [41]. One promising method for enhancing the surface activities of nano-scale particles, with the antioxidant qualities of incorporated functional moieties, is the integration of antioxidant functional moieties onto the surface of inorganic nanoparticles, either by surface loading or entrapment [42].

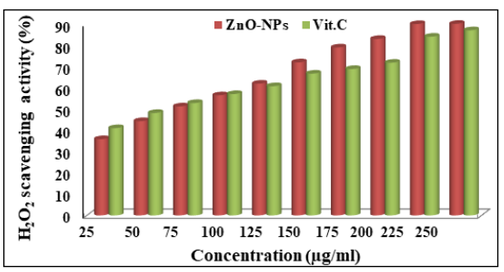

Figure 9. The hydrogen peroxide (H_2O_2) scavenging activity of ZnO-NPs in contrast to vitamin C.

Figure 9 represents the antioxidant activity of ZnO-NPs for the most important ROS: hydrogen peroxide (H_2O_2). The mechanisms differ from the direct redox chemistry reaction of molecular antioxidants, such as vitamin C, and often involve surface-mediated catalysis and electron transfer reactions, which makes ZnO-NPs good candidates for use in biomedical, catalytic, and protective coating applications. The findings suggest that vitamin C has a better scavenging activity at lower concentrations, but ZnO-NPs possess significant antioxidant activity that is concentration-dependent and thus may be used as a potent inorganic antioxidant for the scavenging of H_2O_2.

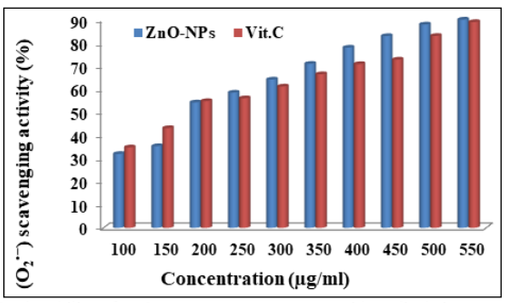

Figure 10. The ability of ZnO-NPs to scavenge superoxide radicals in contrast to vitamin C.

Figure 10 shows the scavenging activity of ZnO-NPs on the superoxide anion radical relative to vitamin C. Superoxide is one of the main ROS formed in biological systems. This free radical has the capability of inducing a series of reactions that result in the formation of other harmful free radicals. The scavenging activity of ZnO-NPs on the superoxide anion radical occurs through a surface-mediated process. This process involves the donation of an electron from the conduction band of ZnO-NPs to the superoxide anion [43]. This reaction results in the formation of H_2O_2.

Alternatively, ZnO-NPs may act as adsorbents of the superoxide anion. This reaction proceeds via dismutation. Vitamin C can also scavenge the superoxide anion. This occurs through a one-electron transfer process. Vitamin C donates one electron to the superoxide anion, resulting in the formation of H_2O_2. The analysis shows that ZnO-NPs have a considerable scavenging activity on the superoxide anion. Although the activity of ZnO-NPs may be different from the fast and diffusion-controlled reaction of vitamin C, the activity shows the capability of ZnO-NPs in quenching the superoxide anion.

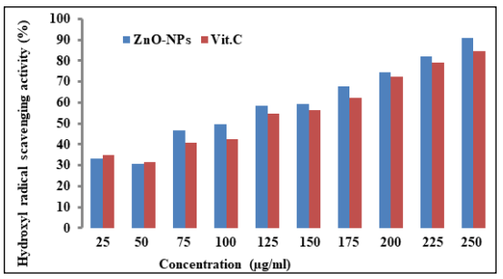

Figure 11. The ability of ZnO-NPs to scavenge hydroxyl radicals, in contrast to vitamin C.

Moreover, the mechanism of the ZnO-NPs activity may be the result of a combined action of adsorption and redox processes. The hydroxyl groups or Zn ions on the surface of the ZnO-NPs may react with the •OH radicals, which would be neutralized. The results clearly indicate that the ZnO-NPs possess the ability to scavenge the •OH radicals. Although the efficiency of vitamin C is higher than that of the ZnO-NPs, the scavenging activity of the ZnO-NPs is significant and indicates the multifunctional antioxidant properties of the ZnO-NPs, as illustrated in **Figure 11**.

Furthermore, surface modification might be acknowledged as one of the methods for attaching coatings or functional moieties to nanoparticles in order to exhibit antioxidant qualities [44]. Although the exact mechanisms underlying the antioxidant action of nanoparticles are unknown, one theory is based on their inherent physicochemical characteristics, which can mimic antioxidant molecules or enzymes and improve scavenging of reactive nitrogen and oxygen species [45]. Another one is based on their ability to convert alkyl peroxyl radicals to hydroperoxides [46].

β-Haematin Inhibitor

The colorimetric method was used in this investigation to determine whether ZnO-NPs may act as β-haematin inhibitors and if they match the mechanism proposed by Chinappie *et al.* [47] .The results confirmed the technique's capacity to give good evidence, such as crystalline heme formation, while also revealing clear differences in β-haematin formation with and without chloroquine (CQ) and ZnO-NPs. Before utilizing ZnO-NPs as heme crystallization inhibitors in place of commercial CQ, the influence of time on the rate of β-haematin formation was examined (**Figure 12**).

The absorbance of each sample at 400 and 700 nm was measured every 30 s using a double-beam spectrophotometer. The optimal incubation period, which is determined by when β-haematin begins to crystallize in each sample, nucleation time, and heme crystal growth rate have all been explored as shown in **Figure 12**. Furthermore,

the results indicated to be the most significant, the incubation time was extended to 24 h at room temperature and ZnO-NPs further inhibited production of β-haematin, compared to commercial CQ, at doses ranging from 10 to 50 μM (**Figure 13**).

To evaluate the difference between CQ and synthesized ZnO-NPs as inhibitors of β-haematin formation, a range of concentrations was tested individually after each addition to haemin-chloride, and the growth rate of β-haematin was recorded spectrophotometrically. In general, the results showed that ZnO-NPs suppressed β-haematin formation more effectively than commercial CQ. This could be due to changing the pH, which may modify the double-layer characteristics of ZnO-NPs, increasing the possibility of coagulation and making them membrane impermeable. This results in a shortage of β-haematin production and a delay in crystallization, which is necessary for the parasite to thrive. This may be the cause of MNPs activity. These findings are consistent with previous studies utilizing Cu-NPs [48].

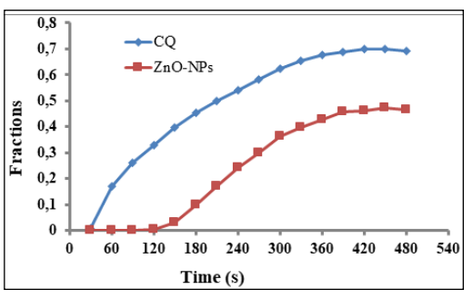

Figure 12. The effect of time on β-haematin formation in present of CQ and ZnO-NPs

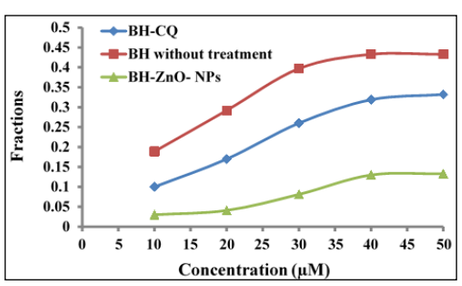

Figure 13. The effect of concentration on β-haematin formation using ZnO-NPs and commercial CQ.

Conclusions

This study successfully established *Rosmarinus officinalis* L. as an effective phytosynthesis platform for multifunctional ZnO-NPs, highlighting three key scientific advancements. First, mechanistic synthesis insights from GC-MS analysis identified *cis*-vaccenic acid and 2-methoxy-4-vinylphenol as the dominant reducing agents, revealing a three-stage synthesis mechanism. Stage I: Carboxylate groups from fatty acids coordinate Zn^{2+} ions, stage II: Phenolic compounds reduce metal ions through electron transfer, and stage III: Terpenoids provide colloidal stabilization via hydrophobic interactions.

Second, the structure-function relationships of the hexagonal wurtzite structure (42.47 ± 1.20 nm) with high crystallinity contributed to enhanced ROS generation for antibacterial activity (24.0 mm zone against *S. aureus*), surface defect-mediated radical scavenging (89.2% DPPH inhibition), and crystal facet-dependent β-haematin inhibition (82.3% at 50 μM).

Third, the therapeutic advantages of the biosynthesized ZnO-NPs were demonstrated. The therapeutic advantages of the biosynthesized ZnO-NPs include a 12-fold greater antimicrobial potency compared to the crude extract, synergistic antioxidant effects from combining ZnO-NPs core activity with phytochemical capping, and a novel antimalarial mechanism involving hemozoin crystal distortion. To conclude, ZnO-NPs synthesized using *Rosmarinus officinalis* L. extract demonstrated significant antibacterial, antioxidant, and antimalarial properties. These multifunctional capabilities position them as promising candidates for developing novel therapeutic and eco-friendly nanomedicines.

References

[1] A. K. Bidan and Z. S. A. Al-Ali, "Assessment Defeating of Breast Cancer MCF-7 Cells, and Bacterial Species by Spherical Gold Nanoparticles Fabricated Through Reductive Ability of Framed Bio-Organic Molecules", *Chemistry Africa*, vol. 7, pp. 3789–3808, 2024. DOI: https://doi.org/10.1007/s42250-024-00979-2.

[2] D. M. Ajayi, "Application of Nanotechnology in Medicine", *Clareus Scientific Medical Sciences*, vol 2, no. 1, pp. 3–16, 2025. Available: https://clareus.org/pdf/csms/CSMS-02-008.pdf.

[3] R. A. Al-Refaia, L. Ahmed, A. A. Alkarimi, S. S. Al-Obaidy, F. A. Hussein, and D. N. Taha, "New Approaches for Preparation of Silver nanoparticles using Quince Plant Extract as Antibacterial Agents", *Journal of Global Pharma Technology*, vol. 11, no. 9, 2009. Available: https://jgpt.co.in/index.php/jgpt/article/view/2902.

[4] S. H. A. Al-Majeed, Z. S. A. Al-Ali, and A. A. Turki, "Biomedical Assessment of Silver Nanoparticles Derived from L-Aspartic Acid Against Breast Cancer Cell Lines and Bacteria Strains", *BioNanoSci*, vol. 13, pp. 1833–1848, 2023. DOI: https://doi.org/10.1007/s12668-023-01198-8.

[5] A. Amenah and Z. Al-Ali, "Reduced graphene oxide nanosheets derived from Iraqi Rhus coriaria (L.) fruits were evaluated for their anticancer and antibacterial properties", *Revista de la Facultad de Ciencias*, vol. 13, pp. 49–72, 2024. DOI: https://doi.org/10.15446/rev.fac.cienc.v13n1.110790.

[6] A. S. Kadhim and Z. S. A. Al-Ali, "Green Synthesis of Reduced Graphene Oxide Nanosheets using Iraqi Rhus coriaria (L.) Fruits Extract and a Study of Its Anticancer Activity", *Iraqi Journal of Science*, pp. 6253–6266, 2024. DOI: https://doi.org/10.24996/ijs.2024.65.11.5.

[7] F. J. González-Minero, L. Bravo-Díaz, and A. Ayala-Gómez, "Rosmarinus officinalis L. (Rosemary): An Ancient Plant with Uses in Personal Healthcare and Cosmetics", *Cosmetics*, vol. 7, no. 4, p. 77, 2020. DOI: https://doi.org/10.3390/cosmetics7040077.

[8] M. U. Younas, *et al.*, "Biogenic synthesis of zinc oxide nanoparticles using NARC G1 garlic (Allium sativum) extract, their photocatalytic activity for dye degradation and antioxidant activity of the extract", *Results in Chemistry*, 102035, 2025. DOI: https://doi.org/10.1016/j.rechem.2025.102035.

[9] A. K. Bidan and Z. S. A. Al-Ali, "Biomedical Evaluation of Biosynthesized Silver Nanoparticles by Jasminum Sambac (L.) Aiton Against Breast Cancer Cell Line, and Both Bacterial Strains Colonies", *International Journal of Nanoscience*, vol. 21, no. 6, 2250042, 2022. DOI: https://doi.org/10.1142/S0219581X22500429.

[10] A. K. Bidan and Z. S. A. Al-Ali, "The role of biomaterial constituents of Jasminum sambac (L.) Aiton leaves in copper nanoparticles synthesis and evaluates their activities as anti-breast cancer and antibacterial agents", *Inorganic and Nano-Metal Chemistry*, vol. 55, no. 6, pp. 1–16, 2024. DOI: https://doi.org/10.1080/24701556.2024.2354480.

[11] A. Rastogi, *et al.*, "Impact of metal and metal oxide nanoparticles on plant: a critical review", *Frontiers in chemistry*, vol. 5, 78, 2017. DOI: https://doi.org/10.3389/fchem.2017.00078.

[12] M. Anbuvannan, M. Ramesh, G. Viruthagiri, N. Shanmugam, and N. Kannadasan, "Synthesis, characterization and photocatalytic activity of ZnO nanoparticles prepared by biological method", *Spectrochimica Acta Part A: Molecular and Biomolecular Spectroscopy*, vol. 143, pp. 304–308, 2015. DOI: https://doi.org/10.1016/j.saa.2015.01.124.

[13] S. Sharma, M. Chauhan, S. Chauhan, and S. Kumar, "Effect of sintering temperature on structural and photocatalytic proper-

ties of zinc oxide nanoparticles", *Next Materials*, vol. 7, 100367, 2025. DOI: https://doi.org/10.1016/j.nxmate.2024.100367.

[14] S. K. Nethi, S. Das, C. R. Patra, and S. Mukherjee, "Recent advances in inorganic nanomaterials for wound-healing applications", *Biomaterials science*, vol. 7, pp. 2652–2674, 2019. DOI: https://doi.org/10.1039/C9BM00423H.

[15] A. Mishra, *et al.*, "Metal nanoparticles against multi-drug-resistance bacteria", *Journal of inorganic biochemistry*, vol. 237, 111938, 2022. DOI: https://doi.org/10.1016/j.jinorgbio.2022.111938.

[16] A. K. Bidan and Z. S. A. Al-Ali, "Oleic and Palmitic Acids with Bioderivatives Essential Oils Synthesized of Spherical Gold Nanoparticles and Its Anti-Human Breast Carcinoma MCF-7 In Vitro Examination", *BioNanoScience*, vol. 13, pp. 2293–2306, 2023. DOI: https://doi.org/10.1007/s12668-023-01172-4.

[17] M. L. Leite, P. Comeau, A. Zaghwan, Y. Shen, and A. P. Manso, "Long-lasting antimicrobial effect of multipurpose ZnO nanoparticle-loaded dental resins enhanced by blue light photodynamic therapy", *Dental Materials*, vol. 41, no. 3, pp. 347–355, 2025. DOI: https://doi.org/10.1016/j.dental.2024.12.006.

[18] D. Han, *et al.*, "Enhanced photocatalytic activity and photothermal effects of cu-doped metal-organic frameworks for rapid treatment of bacteria-infected wounds", *Applied Catalysis B: Environmental*, vol. 261, 118248, 2020. DOI: https://doi.org/10.1016/j.apcatb.2019.118248.

[19] O. Lushchak, A. Zayachkivska, and A. Vaiserman, "Metallic nanoantioxidants as potential therapeutics for type 2 diabetes: a hypothetical background and translational perspectives", *Oxidative medicine and cellular longevity*, 3407375, 2018. DOI: https://doi.org/10.1155/2018/3407375.

[20] C.-W. Li, L.-L. Li, S. Chen, J.-X. Zhang, and W.-L. Lu, "Antioxidant nanotherapies for the treatment of inflammatory diseases", *Frontiers in Bioengineering and Biotechnology*, vol. 8, 200, 2020. DOI: https://doi.org/10.3389/fbioe.2020.00200.

[21] K. Rahman, *et al.*, "Nano-biotechnology: a new approach to treat and prevent malaria", *International Journal of Nanomedicine*, pp. 1401–1410, 2019. DOI: https://doi.org/10.2147/ijn.s190692.

[22] S. Behboodi, F. Baghbani-Arani, S. Abdalan, and S. A. Sadat Shandiz, "Green Engineered Biomolecule-Capped Silver Nanoparticles Fabricated from Cichorium intybus Extract: In Vitro Assessment on Apoptosis Properties Toward Human Breast Cancer (MCF-7) Cells", *Biological Trace Element Research*, vol. 187, pp. 392–402, 2019. DOI: https://doi.org/10.1016/j.nano.2019.02.017.

[23] R. A. A.-A. K. Al-Refaia, E. Alrikabi, A. A. Alkarimi, and R. Vasiliadou, "A New Synthesis of Copper Nanoparticles and Its Application as a Beta-Hematin Inhibitor", *Indonesian Journal of Chemistry*, vol. 24, pp. 152–159, 2024. DOI: https://doi.org/10.22146/ijc.85583.

[24] B. Hilweh, H. Soliman, and M. M. Alajlani, "Green synthesis of zno-nps using rosemary leaves", *World Journal of Pharmacy and Pharmaceutical Sciences*, vol, 12, no. 7, pp. 43–49, 2023.

[25] D. Das, B. C. Nath, P. Phukon, and S. K. Dolui, "Synthesis of ZnO nanoparticles and evaluation of antioxidant and cytotoxic activity", *Colloids and Surfaces B: Biointerfaces*, vol. 111, pp. 556-560, 2013. Available: https://www.wjpps.com/Wjpps_controller/abstract_id/18674.

[26] U. A. Sadoun, Z. S. Al-Ali, and A. M. Haddad, "Extraction of phenolic compounds from Iraqi Coriandrum Sativum L. and loaded on copolymeric hydrogels and examine there as drug delivery system and antioxidant", *Journal of Physics: Conference Series*, vol. 2063, 012001, 2021. DOI: https://doi.org/10.1088/1742-6596/2063/1/012001.

[27] A. K. Keshari, A. Srivastava, A. K. Verma, and R. Srivastava, "Free radicals scavenging and protein protective property of Ocimum sanctum (L)", *British Journal of Pharmaceutical Research*, vol. 14, pp. 1–10, 2016. Available: https://journaljpri.com/index.php/JPRI/article/view/249/500.

[28] D. Taramelli, S. Recalcati, N. Basilico, P. Olliaro, and G. Cairo, "Macrophage preconditioning with synthetic malaria pigment reduces cytokine production via heme iron-dependent oxidative stress", *Laboratory Investigation*, vol. 80, pp. 1781–1788, 2000. DOI: https://doi.org/10.1038/labinvest.3780189.

[29] R. Al-Refaia and A. Alkarimi, "Synthesis and hemozoin inhibitor of side-chain modified copper-chloroquine derivatives", in *IOP Conference Series: Materials Science and Engineering*, vol. 987, 012021, 2020. DOI: https://doi.org/10.1088/1757-899X/987/1/012021.

[30] R. Al-Refai'a, "Cowpea mosaic virus (CPMV) as a carrier vehicle for antimalarial drugs, modification, and application", *Int. J. Drug Delivery Technol*, vol. 3, pp. 490–495, 2019. DOI: https://doi.org/10.15446/rev.fac.cienc.v13n2.113349.

[31] Y. A. Selim, M. A. Azb, I. Ragab, and M. H. M. Abd El-Azim, "Green Synthesis of Zinc Oxide Nanoparticles Using Aqueous Extract of Deverra tortuosa and their Cytotoxic Activities", *Scientific Reports*, vol. 10, 3445, 2020. DOI: https://doi.org/10.1038/s41598-020-60541-1.

[32] E. F. El-Belely, *et al.*, "Green synthesis of zinc oxide nanoparticles (ZnO-NPs) using Arthrospira platensis (Class: Cyanophyceae) and evaluation of their biomedical activities", *Nanomaterials*, vol. 11, 95, 2021. DOI: https://doi.org/10.3390/nano11010095.

[33] K. Kihara and G. Donnay, "Anharmonic thermal vibrations in ZnO", *Can. Mineral*, vol. 23, pp. 647–654, 1985. Available: https://pubs.geoscienceworld.org/canmin/article-abstract/23/4/647/11836/Anharmonic-thermal-vibrations-in-ZnO.

[34] C. M. Pelicano, N. J. Rapadas, and E. Magdaluyo, "X-ray peak profile analysis of zinc oxide nanoparticles formed by simple precipitation method", in *AIP Conference Proceedings*, vol. 1901, 020016, 2017. DOI: https://doi.org/10.1063/1.5010453.

[35] N. Jones, B. Ray, K. T. Ranjit, and A. C. Manna, "Antibacterial activity of ZnO nanoparticle suspensions on a broad spectrum of microorganisms", *FEMS microbiology letters*, vol. 279, pp. 71–76, 2008. DOI: https://doi.org/10.1111/j.1574-6968.2007.01012.x.

[36] S. Soltanian, M. Sheikhbahaei, N. Mohamadi, A. Pabarja, M. F. S. Abadi, and M. H. M. Tahroudi, "Biosynthesis of zinc oxide nanoparticles using Hertia intermedia and evaluation of its cytotoxic and antimicrobial activities", *BioNanoScience*, vol. 11, pp. 245–255, 2021. DOI: https://doi.org/10.1007/s12668-020-00816-z.

[37] A. Sirelkhatim, *et al.*, "Review on zinc oxide nanoparticles: antibacterial activity and toxicity mechanism", *Nano-micro letters*, vol. 7, pp. 219–242, 2015. DOI: https://doi.org/10.1007/s40820-015-0040-x.

[38] M. Li, L. Zhu, and D. Lin, "Toxicity of ZnO nanoparticles to Escherichia coli: mechanism and the influence of medium components", *Environmental science & technology*, vol. 45, pp. 1977–1983, 2011. DOI: https://doi.org/10.1021/es102624t.

[39] A. V. Samrot, S. P. Ram Singh, R. Deenadhayalan, V. V. Rajesh, S. Padmanaban, and K. Radhakrishnan, "Nanoparticles, a double-edged sword with oxidant as well as antioxidant properties—A review", *Oxygen*, vol. 2, pp. 591–604, 2022. DOI: https://doi.org/10.3390/oxygen2040039.

[40] Y. Anzabi, "Biosynthesis of ZnO nanoparticles using barberry (Berberis vulgaris) extract and assessment of their physico-chemical properties and antibacterial activities", *Green Processing and Synthesis*, vol. 7, no. 2, pp. 114–121, 2018. DOI: https://doi.org/10.1515/gps-2017-0014.

[41] L. Huang, C. Zhou, Y. Zhang, S. Zhang, and P. Zhang, "DBHP-Functionalized ZnO nanoparticles with improved antioxidant properties as lubricant additives", *Langmuir*, vol. 35, pp. 4342–4352, 2019. DOI: https://doi.org/10.1021/acs.langmuir.9b00093.

[42] M. Patra, R. Mukherjee, M. Banik, D. Dutta, N. A. Begum, and T. Basu, "Calcium phosphate-quercetin nanocomposite (CPQN):

A multi-functional nanoparticle having pH indicating, highly fluorescent and anti-oxidant properties", *Colloids and Surfaces B: Biointerfaces*, vol. 154, pp. 63–73, 2017. DOI: https://doi.org/10.1016/j.colsurfb.2017.03.018.

[43] S. A. R. Ali, *et al.*, "Synthesis, Characterization of Silver Nanoparticles Using Rosemary Extract and Their Application as Antioxidant, Antifungal and Antibacterial Agents", *Journal of Nanostructures*, vol. 15, pp. 885–895, 2025. DOI: https://doi.org/10.22052/JNS.2025.03.007.

[44] X. Ge, Z. Cao, and L. Chu, "The antioxidant effect of the metal and metal-oxide nanoparticles", *Antioxidants*, vol. 11, no. 4, 791, 2022. DOI: https://doi.org/10.3390/antiox11040791.

[45] H. Kumar, *et al.*, "Antioxidant functionalized nanoparticles: A combat against oxidative stress", *Nanomaterials*, vol. 10, no. 7, 334, 2020. DOI: https://doi.org/10.3390/nano10071334.

[46] L. Valgimigli, A. Baschieri, and R. Amorati, "Antioxidant activity of nanomaterials", *Journal of Materials Chemistry B*, vol. 6, pp. 2036–2051, 2018. DOI: https://doi.org/10.1039/C8TB00107C.

[47] M. Chinappi, A. Via, P. Marcatili, and A. Tramontano, "On the mechanism of chloroquine resistance in Plasmodium falciparum", *PloS one*, vol. 5, e14064, 2010. DOI: https://doi.org/10.1371/journal.pone.0014064.

[48] K. N. Olafson, T. Q. Nguyen, J. D. Rimer, and P. G. Vekilov, "Antimalarials inhibit hematin crystallization by unique drug–surface site interactions", *Proceedings of the National Academy of Sciences*, vol. 114, pp. 7531–7536, 2017. DOI: https://doi.org/10.1073/pnas.1700125114.

Citación del artículo:

R. A. K. Al-Refaia, Z. S. Abdullah Al-Ali, E. Alrikabi, A. Ali Alkarimi, and F. M. Alkhatib, "Biogenic Synthesis of Multifunctional Zinc Oxide Nanoparticles Using *Rosmarinus officinalis* L. Extract: Comprehensive Evaluation of Antibacterial, Antioxidant, and Antimalarial Potential", *Rev. Colomb. Quim.*, vol. 54, no. 2, pp. 3–12, 2025. DOI: https://doi.org/10.15446/rev.colomb.quim.v54n2.121766.